International Journal of All Research Education and Scientific Methods (IJARESM),
ISSN: 2455-6211, Volume 12, Issue 4, April-2024, Available online at: www.ijaresm.com

Design, Synthesis and Pharmacological Evaluation of 1-Phenyl-4,5-Dihydro-1H-Pyrazoles Derivative by in-Vitro and in-Silico Methods: A Combined Approach

Rohit Kumar[1], Ankit Verma[1], Swati Rathore[1], Richa Tripathy[1], Asmita Gajbhiye[1], Shailendra Patil[2]

[1]Department of Pharmaceutical Sciences, Dr. Harisingh Gour Vishwavidyalaya, Sagar, M.P., India
[2] SVN Institute of Pharmaceutical Sciences, Swami Vivekanand University, Sironja, Sagar, M.P., India

----------**********----------

ABSTRACT

1-phenyl-4,5-dihydro-1H-pyrazoles derivative have attracted significant attention in medicinal chemistry due to their diverse pharmacological properties and potential therapeutic applications. The study was performed Firstly, chalcone was prepared from the Claisen Schmidt condensation reactions, further different 1-phenyl-4,5-dihydro-1H-pyrazoles derivative were synthesized from condensation reaction by Knorr Pyrazole synthesis. All the derivatives were characterized by IR spectroscopy and NMR spectroscopy. The biological activities of pyrazole derivatives have been investigated for the antioxidant activity by the DPPH assay and H_2O_2 assay. These derivatives were screened for their anticancer activity in comparison with Nintedanib (a marketed anti-cancer drug) by the ADMET analysis. Furthermore, computational methods, including molecular docking and quantum chemical calculations, have been utilized to predict the binding affinities and molecular interactions of pyrazole derivatives with their respective biological targets. These computational studies aid in understanding the mechanisms of action and guide the design of novel derivatives with improved activities and reduced side effects. As a result, synthesized derivatives hold immense potential as a versatile class of compounds with significant biological activities. Ongoing research in this field is likely to uncover new derivatives with enhanced pharmacological properties, paving the way for the development of novel and effective therapeutics in various medical fields.

Keywords: Pyrazoles, chalcone, antioxidant activity, docking studies, anticancer activity

INTRODUCTION

Oxidative stress refers to an imbalance between the productions of reactive oxygen species (ROS) and the ability of the body's antioxidant defenses to neutralize them. ROS are highly reactive molecules that include free radicals such as superoxide anion (O_2^-), hydroxyl radical (•OH), and non-radical species like hydrogen peroxide (H_2O_2)[(1-4)]. While ROS play essential roles in various cellular processes, excessive production or insufficient removal of these molecules can lead to oxidative stress, which can have detrimental effects on cells, tissues, and biological macromolecules. ROS is generated in the body as natural byproducts of cellular metabolism, especially during processes such as aerobic respiration in mitochondria. Additionally, external factors such as environmental pollutants, radiation, certain drugs, and toxins can contribute to ROS production. Macrophages and neutrophils, part of the immune system, also produce ROS during their defense mechanisms against pathogens. The ROS can damage lipids, proteins, and nucleic acids (DNA and RNA) in cells, leading to impaired cellular functions and potentially contributing to various diseases and aging[(5-12)].

Oxidative stress plays a significant role in the development and progression of cancer. It is a complex interplay between the body's normal cellular processes, the production of reactive oxygen species (ROS), and the body's antioxidant defense mechanisms[(13-15)].While low levels of ROS are essential for various cellular functions, excessive and chronic oxidative stress can contribute to the initiation and promotion of cancer through several mechanisms such as DNA damage and mutation, activation of signaling pathways, promotion of angiogenesis and metastasis, immune suppression, resistance to therapy, tumor microenvironment, genetic and epigenetic alterations[(16-18)].

In the present study, pyrazole derivatives were synthesized with antioxidant activity by incorporating specific functional groups onto the pyrazole ring. These derivatives may scavenge free radicals, inhibit lipid peroxidation, and modulate key antioxidant enzymes. By reducing oxidative stress, pyrazole derivatives could contribute to cellular health and potentially aid in preventing or managing oxidative stress-related diseases. Due to the reduction of oxidative stress, they also prevent the occurrence of cancer as well as in the decrement in the cancer condition[(17-21)].

International Journal of All Research Education and Scientific Methods (IJARESM),
ISSN: 2455-6211, Volume 12, Issue 4, April-2024, Available online at: www.ijaresm.com

Pyrazoles are a class of five-member heterocyclic compounds with a nitrogen atom at position 1 and a carbon-carbon double bond at position 2 and 3. They have garnered significant interest in the field of medicinal chemistry and drug discovery due to their diverse biological activities and therapeutic potential. The general formula of a pyrazole is $C_3H_3N_2$. The two nitrogen atoms in the ring can be in different positions, resulting in two isomeric forms: 1H-pyrazole and 3H-pyrazole. However, the term "pyrazole" is often used to refer to the 1H-pyrazole isomer, which is the most common and widely studied form[22-24].

Many pyrazole derivatives have exhibited a range of biological activities, including antimicrobial, anti-inflammatory, antiviral, antitumor, and enzyme inhibition properties. Various pyrazole derivatives were screened by researchers to modify the pyrazole scaffold to fine-tune these activities and enhance the compound's efficacy and selectivity [25-27].

However, the various derivatives of pyrazole already circulated in pharmaceutical market. In which, some of the compounds specifically designed to exhibit antioxidants as well as anticancer potential to improve or prevent the occurrence of other abnormalities related to the cancer. But, some of the marketed scaffold shows less activity and more side-effects. To overcome these drawbacks, some pyrazole derivatives have been synthesized in the current study. These derivatives show greater efficacy and require potential to treat the calamity[27-28].

MATERIALS AND METHODS

All the chemicals were purchased from the Sigma Aldrich and the reagents were purchased from the Thermofisher Scientific. Pre-coated silica gel-aluminum plates (Merck, F-254) used for thin-layer chromatography (TLC). IR scpectra were obtained from the Bruker FT-IR Spectrophotometer. ^{1}HNMR (500 MHz) spectra were obtained from the JEOL NMR spectrometer. Absorbance was recorded on UV Spectrophotometer. The uncorrected melting point were determined of all the compounds by the melting point apparatus.

Synthesis of 1-(benzo[1,3]dioxol-5-yl)-3-(4-fluorophenyl)prop-2-en-1-one: Take 3,4-methylenedioxy acetophenone (1 mmol; 0.164 gm) and 4-fluorobenzaldehyde (1 mmol; 0.124 gm) in a round bottom flask. Add (5 ml) ethanol to dissolve both the substances followed by stirring for 15 minutes on an ice bath. Then add (1 ml; 50 %) NaOH to it and stir the mixture continuously for 5 hours. The reaction completion was checked by precoated TLC plates n-hexane:ethylacetate (4:1) as mobile phase. After the completion of reaction leave the mixture over the night in refrigerator. Next day, neutralize the reaction mixture by using dilute HCL (40%) and washed thoroughly by distilled water. The product was filtered and recrystallized from ethanol.

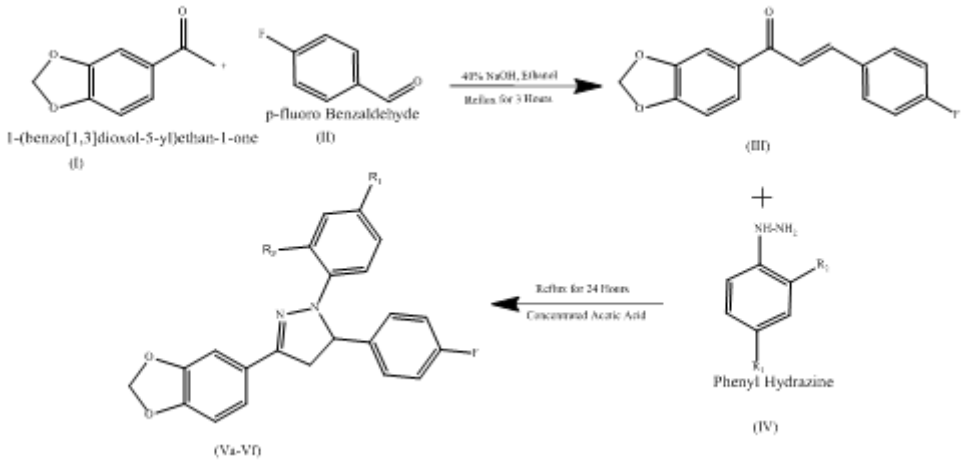

Substitution on R_1 and R_2 in scheme.

Derivatives	Va	Vb	Vc	Vd	Ve	Vf
R_1	H	CH_3	NO_2	F	CN	NO_2
R_2	H	H	H	H	H	NO_2

Figure 1. Synthesis of 3-(benzo[1,3]dioxol-5-yl)-5-(4-fluorophenyl)-1-phenyl-4,5-dihydro-1H-pyrazole derivatives (Va-Vf)

Synthesis of 3-(benzo[1,3]dioxol-5-yl)-5-(4-fluorophenyl)-1-phenyl-4,5-dihydro-1H-pyrazole derivatives (Va-Vf): Take phenyl hydrazine substituted (1mmol) and (E)-1-(benzo[1,3]dioxol-5-yl)-3-(4-fluorophenyl)prop-2-en-1-one (1 mmol) in a round bottom flask. Then add 1.5 ml acetic to the mixture. The reaction mixture was refluxed for 24 hours at 110 °C. The reaction progress was checked by the pre-coated TLC plates by using solvent system n-hexane: ethyl

acetate (8.5:1.5). After the completion of reaction, mixture was poured on ice of distilled water, the product so formed was filtered by using Whatman filter paper and washed with cold distilled water 4-5 times followed by recrystallization from ethanol.

3-(benzo[1,3]dioxol-5-yl)-5-(4-fluorophenyl)-1-phenyl-4,5-dihydro-1H-pyrazole (Va): Orange solid, 65.14%, M.P. 110-112 °C; IR (KBr) cm^{-1}: 1593.19 (C=N), 1495.65 (C=C), 1228.10 (C-O-C), 1030.21 (C-F), 797.96 (C-H, p-substituted), 684.85 (C-H, m-substituted); ^{1}H-NMR (500 MHz, $CdCl_3$) δ 7.692-7.535 (m, 2H, Ar-H), 7.430 (s, 1H, Ar-H) 7.394-7.243 (m, 6H, Ar-H), 6.942-6.872 (m, Ar-2H), 5.31-5.019-5.008, 5.0-4.988 (dd, J = 5.5, 6.0 Hz, pyrazoline-1H), 3.720-3.703 (dd, J = 2.5 Hz, pyrazoline-1H), 2.168-2.080 (dd, J = 20, 17.5 Hz, 1H)

3-(benzo[d][1,3]dioxol-5-yl)-5-(4-fluorophenyl)-1-(p-tolyl)-4,5-dihydro-1H-pyrazole (Vb): Brown solid, 73.44%, M.P. 62-64 °C; IR (KBr) cm^{-1}: 2921.32 (C-H, Methyl), 1598.22 (C=N), 1448.29 (C=C), 1225.51 (C-O-C), 1028.22 (C-F), 926.58 (C-H, p-substituted), 796.33 (C-H, m-substituted); ^{1}H-NMR (500 MHz, $CdCl_3$) δ 7.875-7.753 (dd, J = 12.5, 16.0, 1H, Ar-H), 7.688-7.369(m, 5H, Ar-H) 7.262-7.011 (m, 4H, Ar-H) 6.936-6.859 (dd, J = 8.5, 12.0, Ar-1H), 5.037-4.999, (dd, J = 5.5, 6.0 Hz, pyrazoline-1H), 3.776-3.712 (dd, J = 3.5 Hz, pyrazoline-1H), 3.035-2.995 (dd, J = 7.0 Hz, pyrazoline-1H), 2.297 (s, CH_3-3H)

3-(benzo[d][1,3]dioxol-5-yl)-5-(4-fluorophenyl)-1-(4-nitrophenyl)-4,5-dihydro-1H-pyrazole (Vc): Brown solid, 69.57%, M.P. 70-75 °C; IR (KBr) cm^{-1}: 1596.30 (C=N), 1504.07 (C=C), 1231.87 (C-O-C), 1032.80 (C-F), 795 (C-H, p-substituted), 697 (C-H, m-substituted); ^{1}H-NMR (500 MHz, $CdCl_3$) δ 8.362-8.344 (d, J = 9 Hz, 2H, Ar-H), 7.782-7.707 (dd, J = 10, 15.5 Hz, 1H, Ar-H) 7.644-7.374 (m, 4H, Ar-H) 7.266-6.871 (m, 3H, Ar-H), 5.026-5.010 (dd, J = 3.5, 4.5 Hz, pyrazoline-1H), 3.413-3.365 (dd, J = 6.0, 7.5 Hz, pyrazoline-1H), 3.202-3.145 (dd, J = 7.0 Hz, pyrazoline-1H),

3-(benzo[d][1,3]dioxol-5-yl)-1,5-bis(4-fluorophenyl)-4,5-dihydro-1H-pyrazole (Vd): Brown solid, 61.24%, M.P. 109-111 °C; IR (KBr) cm^{-1}: 1597 (C=N), 1498.86 (C=C), 1230.33 (C-O-C), 1033.90 (C-F), 799.07 (C-H, p-substituted), 709.2 (C-H, m-substituted); ^{1}H-NMR (500 MHz, $CdCl_3$) δ 7.603-7.549 (dd, J = 8.0 Hz 1H, Ar-H), 7.216-7.349 (m, 5H, Ar-H) 7.017-7.013 (m, 4H, Ar-H) 6.012 (s, 1H, Ar-H), 5.128-5.149, (t, J = 5.5, 6.0 Hz, pyrazoline-1H), 3.785-3.735 (dd, J = 6.5 Hz, pyrazoline-1H), 3.075-3.075-3.030 (dd, J = 7.0, 8.0 Hz, pyrazoline-1H)

4-(3-(benzo[d][1,3]dioxol-5-yl)-5-(4-fluorophenyl)-4,5-dihydro-1H-pyrazol-1-yl) benzonitrile (Ve): Orange solid, 58.94%, M.P. 61-63 °C; IR (KBr) cm^{-1}: 2372.31 (CΞN), 1594.06 (C=N), 1501.66 (C=C), 1228.47 (C-O-C), 1032.34 (C-F), 832.29 (C-H, p-substituted); ^{1}H-NMR (500 MHz, $CdCl_3$) δ 7.637-7.737 (d, J = 15.5, 2H, Ar-H), 7.649-7.634 (d, 7.5 Hz, 1H, Ar-H) 7.551-7.506 (dd, J = 22.5 Hz, 2H, Ar-H) 7.463-7.455 (d, J = 6.0 Hz, 1H, Ar-H), 7.206-6.980, (m, J = 13 Hz, 4H, Ar-H), 5.314-5.278 (t, J = 5.5, 6.0 Hz, pyrazoline-1H), 3.867-3.809 (dd, J = 12 Hz, pyrazoline-1H), 3.136-3.090 (dd, J = 6.0, 5.5 Hz, pyrazoline-1H)

3-(benzo[d][1,3]dioxol-5-yl)-1-(2,4-dinitrophenyl)-5-(4-fluorophenyl)-4,5-dihydro-1H-pyrazole (Vf): Red Solid, 71.42%, M.P. 165-167 °C; IR (KBr) cm^{-1}: 1593.85 (C=N), 1497.73 (C=C), 1227.69 (C-O-C), 1027.09 (C-F), 815.16 (C-H, p-substituted), 638.21 (C-H, m-substituted); ^{1}H-NMR (500 MHz, $CdCl_3$) δ 9.444 (s, 1H, Ar-H), 9.146-9.062 (dd, J = 16, 13.5 Hz, 1H, Ar-H), 8.318-8.069 (dd, J = 11, 10 Hz, 1H, Ar-H), 7.912-7.898 (d, J = 7.0 Hz, 1H, Ar-H) 7.619 (s, 1H, Ar-H), 7.509-7.045 (m, 4H, Ar-H), 6.896-6.887 (d, J = 4.5 Hz, 1H, Ar-H), 5.013 (t, J = 1.5 Hz, pyrazoline-1H), 2.611-2.523 (dd, J = 4.0 Hz, pyrazoline-1H), 2.187-2.130 (dd, J = 12.5 Hz, pyrazoline-1H)

IN-VITRO STUDY

Anti-oxidant activity: Here, this method was used to determine the antioxidant activity of pyrazole derivatives. In this method, firstly stokes of different concentration like 20, 40, 60, 80, 100µg has been prepared of all the compounds in methanol. The positive control (by which the drug has been compared) ascorbic acid was taken of similar concentrations as the derivatives. The absorbance of the DPPH with methanol was taken as the negative control. All the absorbance was taken at 517nm (visible region)[4-7]. The % inhibition of all derivatives was measured by using the following formula:

% Inhibition = (A_1-A_0/A_1) *100

Here, A_1 is the absorbance of the negative control;

A_0 is the absorbance of the sample

Reagent: 0.1 mM Diphenyl Picryl Hydrazyl (DPPH) radical in methanol.

Table 1. Percentage Inhibition (%) of pyrazole derivatives by using DPPH scavenging assay at different concentration.

CONCENTRATION (µg/ml)	% Inhibition						
	Va	Vb	Vc	Vd	Ve	Vf	AA*
20.00	85.49	82.05	85.49	81.39	81.69	83.59	96.84
40.00	85.61	82.28	88.59	82.82	82.10	84.96	97.31
60.00	85.97	82.58	91.97	83.00	82.64	86.44	97.44
80.00	87.22	82.94	92.57	83.29	83.77	87.28	97.61
100.00	87.93	83.95	93.16	83.59	84.54	87.63	97.72

IN-SILICO STUDIES

The *in-silico* studies were performed for all the derivatives in comparison to Nintedanib. Nintedanib is a marketed drug that is sold under the brand name **Ofev** and **Vergatef**. It used for non-small cell lung cancer that is related to systemic sclerosis-associated interstitial lung disease, pulmonary fibrosis, and interstitial lung disease with progressive phenotype. This interferes with processes such as fibroblast proliferation, differentiation, and laying down extracellular matrix. It will not improve the condition of IPF (Idiopathic Pulmonary Fibrosis). Nintedanib competitively inhibits receptor tyrosine kinases (RTKs) as well as non-receptor tyrosine kinases. NRTK targets of Nintedanib include Lck (lymphocyte-specific protein tyrosine kinase), Lyn (Tyrosine-protein kinase), and Src (Proto-oncogene tyrosine-protein kinase). Platelet-derived growth factor receptors (PDGFR) 1 and 2, fibroblast growth factor receptors (FGFR) 1, 2, and 3, vascular endothelial growth factor receptors (VEGFR) 1, 2, and 3, and FLT3 are among the RTK targets of Nintedanib. It Inhibits PDGFR, FGFR, and VEGFR, which promote fibroblast proliferation, migration, and transformation, and is the basis for its usage in IPF.

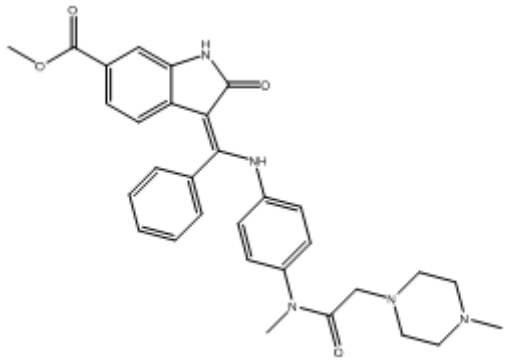

Figure 2. Nintedanib

ADMET Analysis: All the synthesized compounds were analyzed for their ADMET (Absorption Distribution Metabolism Excretion and Toxicity) properties by using an online tool ADMET Lab. The ADMET profile of all the synthesized was compared with Nintedanib (a marketed drug that is used for non-small cell lung cancer). The resultant derivatives exhibit moderate to good ADMET profile in comparison with the marketed drug Nintedanib.

Table 2. The ADMET profile of all the synthesized derivatives in comparison with Nintedanib

Sample	Va	Vb	Vc	Vd	Ve	Vf	Nintedanib
Properties							
LogS	-5.883	-6.192	-5.845	-5.988	-5.945	-5.567	-4.45
LogD	4.577	4.721	4.789	4.521	4.285	4.718	2.823
LogP	5.185	5.601	5.011	5.275	4.828	4.699	3.663
Pgp-inh	0.979	0.999	0.991	0.998	0.849	0.978	1
Pgp-sub	0.002	0.007	0.001	0.002	0.001	0.001	0.086
HIA	0.002	0.002	0.003	0.002	0.004	0.003	0.314

F(20%)	0.002	0.002	0.001	0.001	0.001	0.002	0.071
F(30%)	0.012	0.025	0.003	0.008	0.006	0.001	0.577
Caco-2	-4.873	-4.94	-4.769	-4.874	-4.876	-4.728	-5.613
MDCK	2.8E-05	2.4E-05	4.7E-05	2.5E-05	2.8E-05	0.000326112	1.289E-05
BBB	0.794	0.701	0.267	0.769	0.664	0.188	0.377
PPB	0.9808	0.98466	0.98735	0.9847	0.98718	0.99658638	0.952104
VDss	0.862	0.716	0.563	0.734	0.618	0.68	1.93
Fu	0.02341	0.02527	0.01368	0.02392	0.02942	0.007424985	0.0181216
CYP1A2-inh	0.94	0.805	0.715	0.896	0.751	0.694	0.111
CYP1A2-sub	0.465	0.592	0.19	0.419	0.283	0.187	0.891
CYP2C19-inh	0.943	0.903	0.878	0.873	0.758	0.943	0.3
CYP2C19-sub	0.099	0.133	0.08	0.072	0.071	0.078	0.867
CYP2C9-inh	0.905	0.833	0.918	0.841	0.891	0.961	0.341
CYP2C9-sub	0.901	0.908	0.921	0.906	0.881	0.922	0.172
CYP2D6-inh	0.481	0.16	0.083	0.207	0.019	0.247	0.331
CYP2D6-sub	0.825	0.894	0.858	0.875	0.853	0.802	0.58
CYP3A4-inh	0.925	0.878	0.857	0.868	0.791	0.908	0.749
CYP3A4-sub	0.914	0.925	0.919	0.918	0.925	0.876	0.919
CL	8.474	8.039	5.715	8.131	7.607	3.758	6.684
T12	0.135	0.091	0.076	0.05	0.097	0.066	0.055
hERG	0.089	0.111	0.21	0.166	0.405	0.225	0.981
H-HT	0.175	0.154	0.118	0.317	0.921	0.133	0.47
DILI	0.916	0.905	0.938	0.872	0.922	0.936	0.978
Ames	0.766	0.845	0.965	0.86	0.915	0.977	0.404
ROA	0.129	0.153	0.235	0.122	0.217	0.514	0.468
FDAMDD	0.885	0.904	0.909	0.942	0.951	0.888	0.87
SkinSen	0.104	0.113	0.653	0.083	0.066	0.922	0.213
Carcinogenicity	0.851	0.865	0.912	0.86	0.87	0.911	0.202
EC	0.003	0.003	0.003	0.003	0.003	0.003	0.003
EI	0.035	0.032	0.05	0.028	0.026	0.037	0.006
Respiratory	0.76	0.671	0.876	0.611	0.872	0.863	0.645
BCF	2.838	2.839	2.86	2.721	2.858	2.835	0.55
IGC50	5.046	5.092	5.082	5.06	5.037	5.147	3.326
LC50	6.1	6.245	6.568	6.318	6.323	6.71	4.377
LC50DM	6.176	6.449	6.649	6.891	6.573	6.537	4.454
NR-AR	0.474	0.418	0.33	0.065	0.255	0.086	0.006
NR-AR-LBD	0.148	0.076	0.355	0.104	0.122	0.816	0.098
NR-AhR	0.953	0.954	0.946	0.944	0.94	0.943	0.932
NR-Aromatase	0.592	0.611	0.772	0.687	0.833	0.821	0.311
NR-ER	0.917	0.908	0.901	0.706	0.815	0.838	0.463
NR-ER-LBD	0.028	0.062	0.403	0.014	0.14	0.572	0.007
NR-PPAR-gamma	0.009	0.007	0.049	0.014	0.027	0.407	0.091
SR-ARE	0.677	0.795	0.857	0.744	0.79	0.894	0.384
SR-ATAD5	0.856	0.894	0.682	0.407	0.757	0.661	0.829

SR-HSE	0.429	0.423	0.393	0.456	0.342	0.569	0.005
SR-MMP	0.668	0.639	0.89	0.667	0.713	0.941	0.367
SR-p53	0.618	0.692	0.843	0.62	0.839	0.906	0.846
MW	356.15	370.17	401.14	374.14	381.15	446.12	539.25
Vol	376.791	394.087	402.732	382.859	399.811	428.673	557.82
Dense	0.945	0.939	0.996	0.977	0.953	1.041	0.967
nHA	4	4	7	4	5	10	9
nHD	0	0	0	0	0	0	2
TPSA	34.06	34.06	77.2	34.06	57.85	120.34	94.22
nRot	3	3	4	3	3	5	9
nRing	5	5	5	5	5	5	5
MaxRing	9	9	9	9	9	9	9
nHet	4	4	7	5	5	10	9
fChar	0	0	0	0	0	0	0
nRig	27	27	28	27	28	29	32
Flex	0.111	0.111	0.143	0.111	0.107	0.172	0.281
nStereo	1	1	1	1	1	1	0
Non-Genotoxic_Carcinogenicity	0	0	0	1	0	0	0
LD50_oral	0	0	0	0	0	0	0
Genotoxic_Carcinogenicity_Mutagenicity	1	1	6	1	1	6	1
SureChEMBL	0	0	0	0	0	2	0
NonBiodegradable	0	0	2	1	0	2	1
Skin_Sensitization	1	1	1	1	1	1	7
Acute_Aquatic_Toxicity	0	0	0	1	0	0	3
Toxicophores	2	2	4	2	3	4	4
QED	0.656	0.62	0.455	0.63	0.644	0.404	0.35
Synth	2.585	2.635	2.768	2.651	2.775	2.983	2.609
Fsp3	0.174	0.208	0.174	0.174	0.167	0.174	0.258
MCE-18	77.333	80.172	83.778	80.556	80.357	90.222	63.949
Natural Product-likeness	-1.012	-0.922	-1.241	-1.242	-1.262	-1.156	-1.128
Alarm_NMR	1	1	2	1	1	2	3
BMS	0	0	0	0	0	0	0
Chelating	0	0	0	0	0	0	0
Lipinski	Accepted	Accepted	Accepted	Accepted	Accepted	Accepted	Accepted
Pfizer	Rejected	Rejected	Accepted	Rejected	Rejected	Accepted	Accepted
GSK	Rejected	Rejected	Rejected	Rejected	Rejected	Rejected	Rejected
GoldenTriangle	Accepted	Accepted	Accepted	Accepted	Accepted	Accepted	Rejected

Nintedanib was rejected according to the GSK rule as well as the Golden Triangle rule and accepted according to the Lipinski rule and Pfizer rule only. In our synthesized derivatives all the derivatives follow the Lipinski rule and Golden Triangle rule (Compounds satisfying the golden triangle rule have a more favourable ADMET profile). In all the derivatives **Vc and Vf** were also accepted by the Pfizer rule.The Brain Or IntestinaL EstimateD permeation method (BOILED-Egg) is the best predictive model for computing the lipophilicity and polarity of small molecules. The diagram of boiled egg plotted against WLOGP (n-Octanol/Water coefficient) and TPSA (Topological Polar Surface Area). Because the most populated area of the well-absorbed molecule is elliptical, that's why it is called Egan Egg. The boiled egg exhibits the probability of the molecule to signify the absorption of the molecule by the GIT (Gastrointestinal tract) and permeation through the blood-brain barrier.

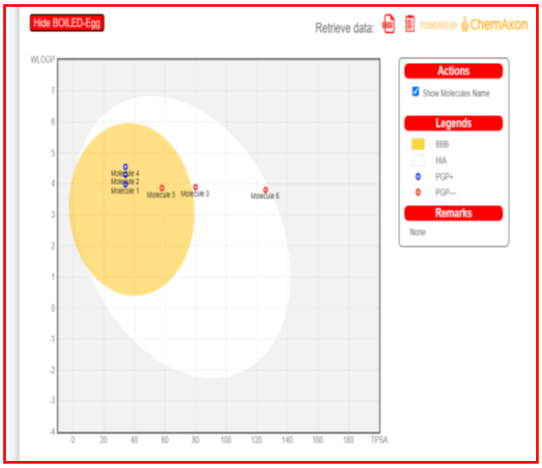

Figure 3. The boiled egg diagram of synthesized derivatives (Va, Vb, Vc, Vd, Ve, and Vf)

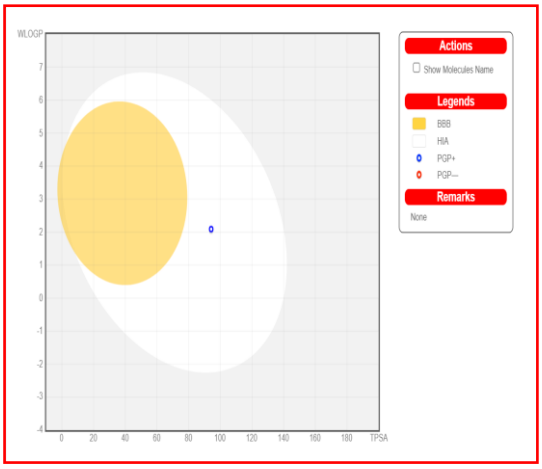

The boiled egg diagram of Nintedanib

The white region is the physicochemical space that signifies the highest probability of the molecule being permeable through GIT whereas the yellow region is the physicochemical space of compounds with the highest probability for permeation through BBB (Blood-Brain Barrier).

Docking Studies: All the synthesized derivatives were docked by using the online tool CB-Dock which was designed by the experts of Auto-dock Vina. The synthesized derivatives were docked on the non-small cell lung cancer protein (6NEC RET PROTEIN TYROSINE KINASE DOMAIN IN COMPLEX WITH NINTEDANIB). This protein was taken from the rcsb.org website. The docking was performed in comparison with **Nintedanib.**

After docking, all the derivatives including Nintedanib visualized by Biovia Discovery Studio and determine the bond distance and their types of interaction between the amino acid and ligand atoms. This information generates a hypothetical approach to determine the exact response of ligand in response to amino acid present at cancer infected organ and to trigger some immunological response to generate or inhibit different type of mediators like interleukin, interferons growth factors, arachidonic acid, eicosanoids etc.

International Journal of All Research Education and Scientific Methods (IJARESM),
ISSN: 2455-6211, Volume 12, Issue 4, April-2024, Available online at: www.ijaresm.com

According to docking, all the derivatives show a moderate to good vina score than the Nintedanib. In all the synthesized derivatives, compound **Vc and Vf** showed the best vina score which was **-0.8 and -11.2**.
As discussed, earlier Nintedanib has less vina score than all the synthesized derivatives which was **-8.9.**
The synthesized derivative **Vb, Vd, Ve and Vf** also showed good vina score at the first possible binding site which was **-10.2, -10.6, -10.6 and -11.2** respectively. The more favorable docking site for all the compounds containing the highest vina scores in comparison with Nintedanib have been shown below:

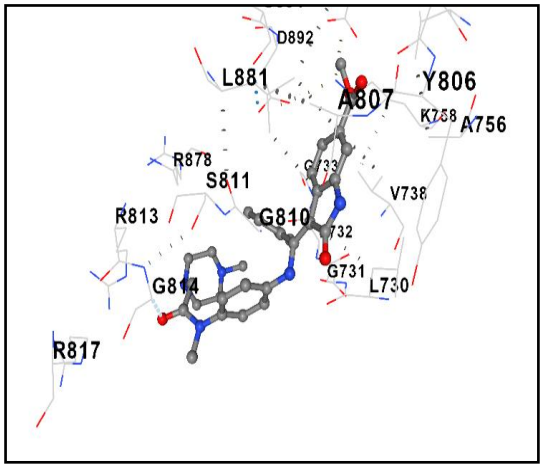

Figure 5. First possible site with vina score -8.9 (Nintedanib)

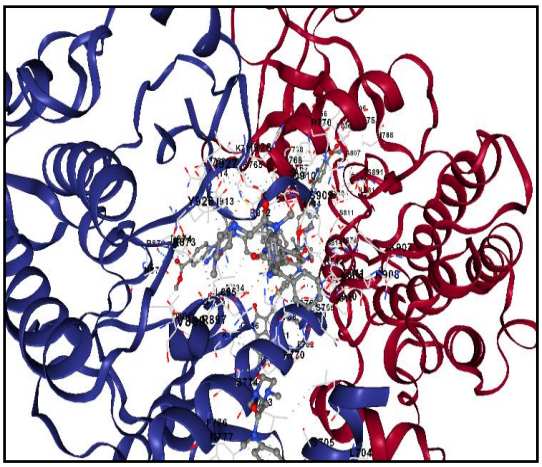

All the possible sites of Nintedanib for 6NEC protein

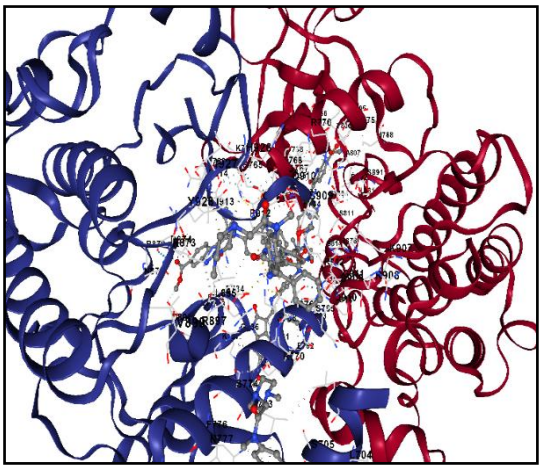

Best possible binding site for synthesized derivatives

International Journal of All Research Education and Scientific Methods (IJARESM),
ISSN: 2455-6211, Volume 12, Issue 4, April-2024, Available online at: www.ijaresm.com

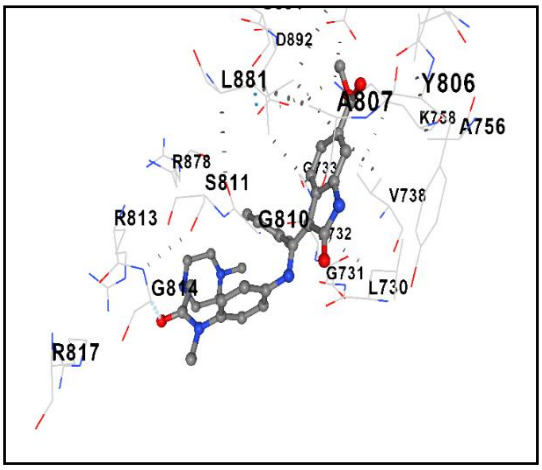

Five best possible cavity for binding of drug to 6NEC tyrosine kinase

RESULT AND DISCUSSION

ADMET Analysis: In our synthesized derivatives all the derivatives follow the Lipinski rule and Golden Triangle rule (Compounds satisfying the golden triangle rule have a more favorable ADMET profile). In all the derivatives **Vc and Vf** were also accepted by the Pfizer rule. According to the boiled egg diagram analysis, the synthesized derivatives **Va, Vb, and V_d** are more permeable to cross (Blood-Brain Barrier), the compound **Vc** shows similar permeability to nintedanib for crossing the BBB. The synthesized derivatives **Vc and Vf** showed good GIT (Gastrointestinal tract) absorption similar to nintedanib which also showed a well GIT absorption probability.

Docking Study: According to docking, all the derivatives showed moderate to good vina score than the nintedanib. In all the synthesized derivatives, compound **Vc and Vf** showed the best vina score which was **-10.8. and -11.2**.
The details of interaction of different types of interaction with amino acid with bond distance shown in table below.

Table 3. The docking score, amino acid, type interaction, bond distance has been shown.

Derivatives	Docking Score	Amino acid interaction	Type of interaction	Bond Distance(Å)
Va	-10.1	Arg878	Fluorine	2.78
		Leu881	Pi-sigma	3.68
		Ser 891	**Pi-Donor H bond**	4.03
Vb	-10.2	Arg892, Lys758	**Conventional H bond**	3.33, 2.95
		Ser811	**Carbon H bond**	3.33
Vc	-10.8	Asp892, Lys758	**Conventional H bond**	3.23, 3.07
		Ser891, Ser811	**Carbon H bond**	3.74, 3.54
		Arg878	Fluorine	3.05
Vd	-10.6	Arg878	Fluorine	2.81
		Ser891	**Pi-Donor H bond**	3.93
		Asp892	Fluorine	3.62
Ve	-10.8	Arg878	Fluorine	2.82
		Ser891	**Pi-Donor H bond**	3.91
		Leu881	Pi-sigma	3.75
Vf	-11.2	Gly731	**Carbon H bond**	3.05
		Glu732, Ser891	**Conventional H bond**	3.12, 3.01
		Asp892	Fluorine	3.04
Nintedanib	-8.9	Arg912, Asp874	**Conventional H bond**	2.50, 2.72
		Glu732, Glu768	**Carbon H bond**	3.60, 3.71

As discussed earlier, nintedanib has less vina score than all the synthesized derivatives which was **-8.9.** In all the synthesized derivative **Vb, Vd, Ve, and Vf** also shows good vina score at the first possible binding site which was **-10.2, -10.6, -10.6 and -11.2** respectively. The main amino acid interaction had less bond distance which may be responsible for the activity.

ANTIOXIDANT ACTIVITY

DPPH (2,2-diphenyl-1-picrylhydrazyl) Scavenging Assay: In synthesized derivatives, the average % inhibition was found to be 86.44, 82.75, 90.35, 82.81, 82.94, and 85.98 of the derivatives **Va, Vb, Vc, Vd, Ve, and Vf**. The average percentage inhibition of Ascorbic acid was found to be 97.38335046. In all of the above derivatives, compound **Vc** had shown excellent % inhibition in comparison to ascorbic acid. All other derivatives also showed good % inhibition.

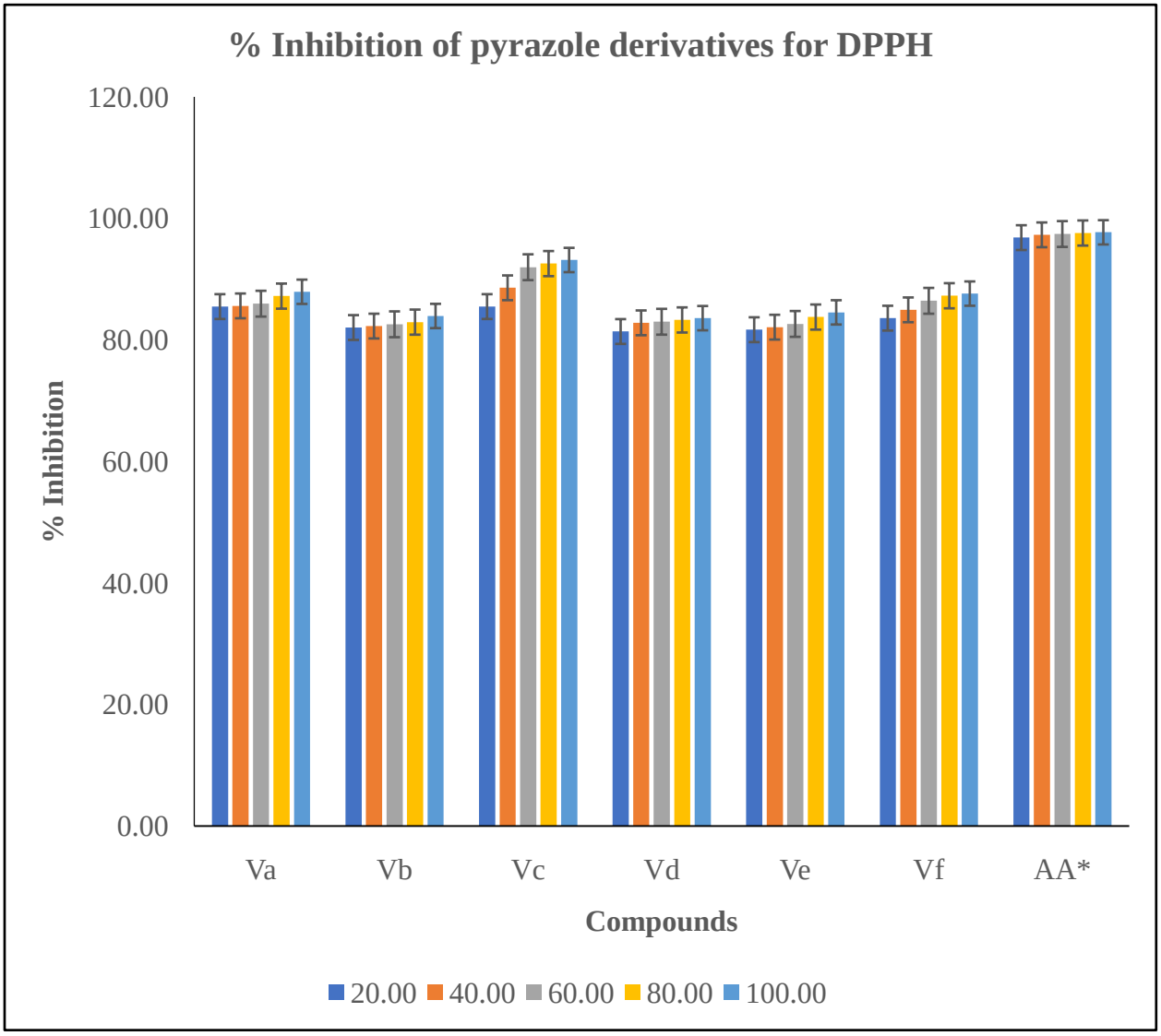

Figure 9. The % Inhibition of pyrazole derivatives in the DPPH assay at different concentrations

Here,
Va =3-(benzo[1,3]dioxol-5-yl)-5-(4-fluorophenyl)-1-phenyl-4,5-dihydro-1H-pyrazole
Vb =3-(benzo[1,3]dioxol-5-yl)-5-(4-fluorophenyl)-1-(p-tolyl)-4,5-dihydro-1H-pyrazole
Vc =3-(benzo[1,3]dioxol-5-yl)-5-(4-fluorophenyl)-1-(4-nitrophenyl)-4,5-dihydro-1H-pyrazole
Vd =3-(benzo[1,3]dioxol-5-yl)-1,5-bis(4-fluorophenyl)-4,5-dihydro-1H-pyrazole
Ve =4-(3-(benzo[1,3]dioxol-5-yl)-5-(4-fluorophenyl)-4,5-dihydro-1H-pyrazol-1-yl)benzonitrile
Vf =3-(benzo[1,3]dioxol-5-yl)-1-(2,4-dinitrophenyl)-5-(4-fluorophenyl)-4,5-dihydro-1H-pyrazole
The IC_{50} of all the derivatives were calculated by the % inhibition of the DPPH assay from the online available tool **AAT Bioquest** IC_{50} Calculator.

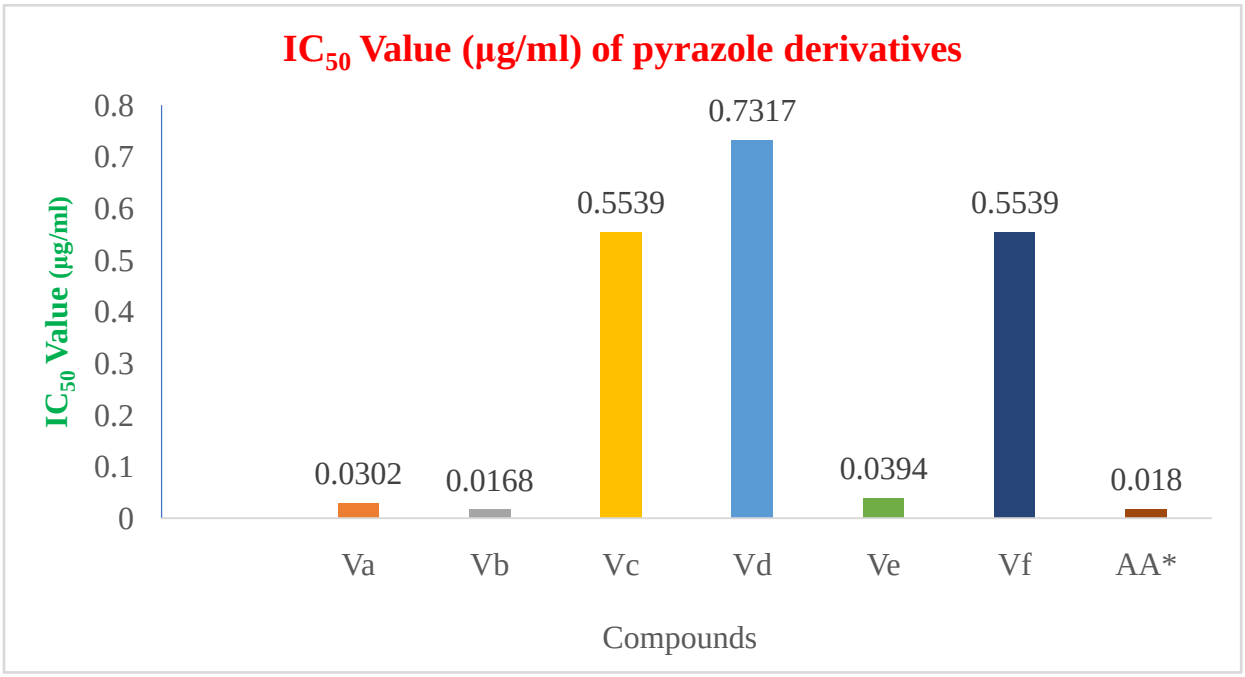

Figure 10. The IC_{50} values of pyrazole derivatives against the standard Ascorbic acid*.

All the synthesized derivatives **Va, Vb, Vc, Vd, Ve, and Vf** showed good IC_{50} values i.e. 0.0302, 0.0168, 0.5539, 0.7317, 0.0394, and 0.5539 (µg/ml) respectively. But compound **Vb** showed an excellent IC_{50} value that was 0.0168 (µg/ml) and standard ascorbic acid that was 0.018 (µg/ml). The compound **Va,** and **Ve** also showed good IC_{50} value.

CONCLUSION

The synthesized derivatives were studied for their ADMET profile against a marketed drug nintedanib. All derivatives showed good ADMET profile than the standard compound nintedanib. The synthesized derivatives further analyzed for their binding affinity with 6NEC (non-small cell lung cancer protein) by docking in comparison with nintedanib. The synthesized derivatives showed good vina score as well as good interaction with lesser bond distance. All the synthesized derivatives were screened for the *in-vitro* antioxidant activity by DPPH scavenging assay by taking ascorbic acid as standard. The % inhibitions of all the derivatives were calculated. In synthesized derivatives, the percentage inhibition of **Vc** was good i.e. 90.35% as compared to standard ascorbic acid that was 97.38%. The IC_{50} of all the derivatives were also calculated against the AA*(ascorbic acid). Compound **Vb** showed an excellent IC_{50} value that was 0.016(µg/ml) than standard ascorbic acid which was 0.018 (µg/ml). The compound **Va** and **Ve** also showed a good IC_{50} Value. From the observation of IC_{50}value of compound **Vb** which contains a methyl substitution on aromatic para-position which was attached to the pyrazole nucleus increase the antioxidant activity of the synthesized derivative. We can conclude from the above results that; the synthesized derivatives have the greater affinity as antioxidant. Based on docking and ADMET analysis, all the synthesized derivatives showed good anticancer activity as compared to that of standard **nintedanib**. This may act as a good pharmacophore for the development of anticancer drugs with good binding affinity as well as greater bond interaction of protein with ligand in the future.

Acknowledgement: The authors are thankful to DST-FIST, New Delhi, SIC facilities and Department of Pharmaceutical Sciences, Dr. Harisingh Gour University, Sagar (M.P.) for all the necessary support. One of the author Mr. Rohit Kumar received financial support from AICTE as JRF from December 2021 to November 2023.

Conflict Of Interest: "No potential conflict of interest relevant to this article was reported."

Funding: One of the author received JRF from AICTE and required chemicals & materials from Department of Pharmaceutical Sciences, Dr. Harisingh Gour University, Sagar (M.P.)

REFERENCES

[1]. Al-Saheb R, Makharza S, Al-Battah F, Abu-El-Halawa R, Kaimari T, Abu Abed OS. Synthesis of new pyrazolone and pyrazole-based adamantyl chalcones and antimicrobial activity. Biosci Rep. 2020;40(9).
[2]. Badgujar JR, More DH, Meshram JS. Synthesis, Antimicrobial and Antioxidant Activity of Pyrazole Based Sulfonamide Derivatives. Indian J Microbiol. 2018;58(1):93–9.

[3]. Bandgar BP, Gawande SS, Bodade RG, Gawande NM, Khobragade CN. Synthesis and biological evaluation of a novel series of pyrazole chalcones as anti-inflammatory, antioxidant and antimicrobial agents. Bioorg Med Chem. 2009;17(24):8168–73.
[4]. Bandgar BP, Gawande SS, Bodade RG, Gawande NM, Khobragade CN. Synthesis and biological evaluation of a novel series of pyrazole chalcones as anti-inflammatory, antioxidant and antimicrobial agents. Bioorg Med Chem. 2009;17(24):8168–73.
[5]. Bhale PS, Bandgar BP, Dongare SB, Shringare SN, Sirsat DM, Chavan H V. Ketene dithioacetal mediated synthesis of 1,3,4,5-tetrasubstituted pyrazole derivatives and their biological evaluation. Phosphorus Sulfur Silicon Relat Elem. 2019;194(8):843–9.
[6]. Brahmbhatt H, Molnar M, Pavić V. Pyrazole nucleus fused tri-substituted imidazole derivatives as antioxidant and antibacterial agents. Karbala International Journal of Modern Science. 2018;4(2):200–6.
[7]. Bugarinović JP, Pešić MS, Minić A, Katanić J, Ilić-Komatina D, Pejović A, et al. Ferrocene-containing tetrahydropyrazolopyrazolones: Antioxidant and antimicrobial activity. J Inorg Biochem. 2018;189:134–42.
[8]. Capaldo L, Ravelli D. Alkoxy radicals generation: Facile photocatalytic reduction of: N -alkoxyazinium or azolium salts. Chemical Communications. 2019;55(21):3029–32.
[9]. Chkirate K, Fettach S, Karrouchi K, Sebbar NK, Essassi EM, Mague JT, et al. Novel Co(II) and Cu(II) coordination complexes constructed from pyrazole-acetamide: Effect of hydrogen bonding on the self assembly process and antioxidant activity. J Inorg Biochem. 2019;191:21–8.
[10]. Elgemeie GH, Abu-Zaied MA, Mossa ATH. Novel Synthesis and Biological Evaluation of the First Pyrazole Thioglycosides as Pyrazofurin Analogues. Nucleosides Nucleotides Nucleic Acids. 2019;38(3):183–202.
[11]. Farag AM, Fahim AM. Synthesis, biological evaluation and DFT calculation of novel pyrazole and pyrimidine derivatives. J Mol Struct. 2019;1179:304–14.
[12]. Faria JV, Vegi PF, Miguita AGC, dos Santos MS, Boechat N, Bernardino AMR. Recently reported biological activities of pyrazole compounds. Bioorganic and Medicinal Chemistry. Elsevier Ltd; 2017. p. 5891–903.
[13]. Gressler V, Moura S, Flores AF, Flores DC, Colepicolo P, Pinto E. Antioxidant and antimicrobial properties of 2-(4, 5-dihydro-1H-pyrazol-1-yl)-pyrimidine and 1-carboxamidino-1H-pyrazole derivatives. Journal of the Brazilian Chemical Society. 2010;21:1477-83.
[14]. Gupta D. METHODS FOR DETERMINATION OF ANTIOXIDANT CAPACITY: A REVIEW. Int J Pharm Sci Res [Internet]. 2015;6(2):546.
[15]. Hamama WS, Gouda MA, Kamal El-din HA, Zoorob HH. Synthesis and Antioxidant Activity of Some New Binary Pyrazoles Containing Core Phenothiazine Moiety. J Heterocycl Chem. 2017;54(2):1369–77.
[16]. Hayyan M, Hashim MA, Alnashef IM. Superoxide Ion: Generation and Chemical Implications. Chemical Reviews. American Chemical Society; 2016. p. 3029–85.
[17]. Hegde H, Ahn C, Shwetha D, Gaonkar SL, Shetty NS. Synthesis of new pyrazoline derivatives and its antimicrobial and antioxidant activities. Journal of the Korean Chemical Society. 2017;61(5):291–5.
[18]. Jeeva JS, Sunitha J, Ananthalakshmi R, Rajkumari S, Ramesh M, Krishnan R. Enzymatic antioxidants and its role in oral diseases. Journal of Pharmacy and Bioallied Sciences. Wolters Kluwer Medknow Publications; 2015. p. S331–3.
[19]. Küçükgüzel G, ŞenkardeŞ S. Recent advances in bioactive pyrazoles. European Journal of Medicinal Chemistry. Elsevier Masson SAS; 2015. p. 786–815.
[20]. Kumara K, Prabhudeva MG, Vagish CB, Vivek HK, Lokanatha Rai KM, Lokanath NK, et al. Design, synthesis, characterization, and antioxidant activity studies of novel thienyl-pyrazoles. Heliyon. 2021;7(7).
[21]. Macarini AF, Sobrinho TUC, Rizzi GW, Corrêa R. Pyrazole–chalcone derivatives as selective COX-2 inhibitors: design, virtual screening, and in vitro analysis. Medicinal Chemistry Research. 2019;28(8):1235–45.
[22]. Martínez MC, Andriantsitohaina R. Reactive nitrogen species: Molecular mechanisms and potential significance in health and disease. Antioxidants and Redox Signaling. Mary Ann Liebert Inc.; 2009. p. 669–702.
[23]. Meador RI, Mate NA, Chisholm JD. Acid Catalyzed N-Alkylation of Pyrazoles with Trichloroacetimidates. Organics. 2022;3(2):111-21.
[24]. Padmaja A, Rajasekhar C, Muralikrishna A, Padmavathi V. Synthesis and antioxidant activity of oxazolyl/thiazolylsulfonylmethyl pyrazoles and isoxazoles. Eur J Med Chem. 2011;46(10):5034–8.
[25]. Pal D, Saha S. (2019) Chondroitin: a natural biomarker with immense biomedical applications. *RSC. Adv*. 9(48): 28061–28077.
[26]. Parmar N, Teraiya S, Patel R, Barad H, Jajda H, Thakkar V. Synthesis, antimicrobial and antioxidant activities of some 5-pyrazolone based Schiff bases. Journal of Saudi Chemical Society. 2015 Jan 1;19(1):36-41.
[27]. Rangaswamy J, Kumar HV, Harini ST, Naik N. Functionalized 3-(benzofuran-2-yl)-5-(4-methoxyphenyl)-4,5-dihydro-1H-pyrazole scaffolds: A new class of antimicrobials and antioxidants. Arabian Journal of Chemistry. 2017;10:S2685–96.
[28]. Sankappa Rai U, Isloor AM, Shetty P, Pai KSR, Fun HK. Synthesis and in vitro biological evaluation of new pyrazole chalcones and heterocyclic diamides as potential anticancer agents. Arabian Journal of Chemistry. 2015;8(3):317–21.

[29]. Santosh R, Selvam MK, Kanekar SU, Nagaraja GK. Synthesis, Characterization, Antibacterial and Antioxidant Studies of Some Heterocyclic Compounds from Triazole-Linked Chalcone Derivatives. ChemistrySelect. 2018;3(23):6338–43.
[30]. Shaik A, Bhandare RR, Palleapati K, Nissankararao S, Kancharlapalli V, Shaik S. Antimicrobial, antioxidant, and anticancer activities of some novel isoxazole ring containing chalcone and dihydropyrazole derivatives. Molecules. 2020;25(5).
[31]. Sharath V, Kumar HV, Naik N. Synthesis of novel indole based scaffolds holding pyrazole ring as anti-inflammatory and antioxidant agents. J Pharm Res. 2013;6(7):785–90.
[32]. Sroka Z, Cisowski W. Hydrogen peroxide scavenging, antioxidant and anti-radical activity of some phenolic acids. Food and Chemical Toxicology. 2003;41(6):753–8.
[33]. Thangarasu P, Manikandan A, Thamaraiselvi S. Discovery, synthesis and molecular corroborations of medicinally important novel pyrazoles; drug efficacy determinations through in silico, in vitro and cytotoxicity validations. Bioorg Chem. 2019;86:410–9.
[34]. Thendral TM, Shafi SS. Design and Synthesis of novel Chalcone Derivatives and their Antioxidant Activity. IOSR Journal of Pharmacy and Biological Sciences (IOSR-JPBS). 13(5):25–8.
[35]. Voskienė A, Mickevičius V. Cyclization of chalcones to isoxazole and pyrazole derivatives, Translated from Khimiya Geterotsiklicheskikh Soedinenii. 2009.